

Linguistics-Vision Monotonic Consistent Network for Sign Language Production

Xu Wang¹, Shengeng Tang^{1*}, Peipei Song², Shuo Wang², Dan Guo¹, Richang Hong¹

¹ School of Computer Science and Information Engineering, Hefei University of Technology, Hefei, China

² School of Information Science and Technology, University of Science and Technology of China, Hefei, China

Abstract—Sign Language Production (SLP) aims to generate sign videos corresponding to spoken language sentences, where the conversion of sign Glosses to Poses (G2P) is the key step. Due to the cross-modal semantic gap and the lack of word-action correspondence labels for strong supervision alignment, the SLP suffers huge challenges in linguistics-vision consistency. In this work, we propose a Transformer-based Linguistics-Vision Monotonic Consistent Network (LVMCN) for SLP, which constrains fine-grained cross-modal monotonic alignment and coarse-grained multimodal semantic consistency in language-visual cues through Cross-modal Semantic Aligner (CSA) and Multimodal Semantic Comparator (MSC). In the CSA, we constrain the implicit alignment between corresponding gloss and pose sequences by computing the cosine similarity association matrix between cross-modal feature sequences (*i.e.*, the order consistency of fine-grained sign glosses and actions). As for MSC, we construct multimodal triplets based on paired and unpaired samples in batch data. By pulling closer the corresponding text-visual pairs and pushing apart the non-corresponding text-visual pairs, we constrain the semantic co-occurrence degree between corresponding gloss and pose sequences (*i.e.*, the semantic consistency of coarse-grained textual sentences and sign videos). Extensive experiments on the popular PHOENIX14T benchmark show that the LVMCN outperforms the state-of-the-art.

Index Terms—Sign Language Production, Cross-modal Semantic Alignment, Multimodal Semantic Comparison.

I. INTRODUCTION

Sign language production plays a significant role in the deaf community as a rich form of visual language communication. Early works focus on avatar-based [1] and statistical machine translation methods [2]. Recently, influenced by the excellence of deep learning, approaches based on CNN&RNN [3]–[6], GAN [7], [8] and VAE [9], [10] have emerged. Nowadays, a new common approach is to employ the Transformer framework to decode pose sequences [11]–[17].

Existing methods suffer huge multi-model semantic gaps due to the lack of robust supervised cross-modal alignment labeling. Although cross-modal semantic consistency has been noted in sign language translation [18]–[21], it has not been addressed in SLP, which needs to generate complex visual semantics from weak text. Nowadays, in many downstream tasks such as cross-modal retrieval [22]–[26], vision-language understanding [27]–[30], multimodal sentiment analysis [31]–[35], researchers tackle the rich multimodal data through the alignment and comparison of cross-modal semantics.

Therefore, we propose a Linguistics-Vision Monotonic Consistent Network (LVMCN) for SLP, which constrains sign linguistic-visual cues from both fine-grained cross-modal monotonic alignment and coarse-grained multimodal semantic consistency. As shown in Figure 1, the LVMCN is designed based on a Transformer framework that consists of a Cross-modal Semantic Aligner and a Multimodal Semantic Comparator. Firstly, the textual and visual semantic features considered as original gloss and pose sequences are extracted from gloss encoder and pose decoder of LVMCN respectively. Next, the semantic features obtained above are simultaneously inputted into the CSA and MSC. We automatically constrain the implicit alignment between the corresponding gloss and pose sequences by calculating the cosine similarity correlation matrices to solve the problem of inconsistent semantics of sign glosses and actions. Meanwhile, we construct multimodal triples from paired and unpaired batch data samples in the MSC. Semantic co-occurrence between gloss and pose sequences is enhanced by aligning corresponding text-visual pairs and separating non-corresponding ones, further improving the consistency of multimodal cues in SLP.

Compared with previous approaches, our main contributions are summarised below: (1) The proposed CSA constructs monotonic alignment of fine-grained cross-modal sequences in forward (linguistics-to-vision) and reverse (vision-to-linguistics). (2) The designed MSC constructs multimodal triples according to the sentence-video matching relationships in the sample data to constrain semantic consistency between coarse-grained textual sentences and sign videos within batch data. (3) The constructed framework incorporates alignment loss \mathcal{L}_{ali} and comparison loss \mathcal{L}_{com} , in conjunction with classical fitting loss \mathcal{L}_{acc} , to jointly optimize the SLP task.

II. METHOD

As illustrated in Figure 1, we proposed LVMCN is constructed based on a Transformer framework (see Section II-A), which includes two key modules: Cross-modal Semantic Aligner (CSA) (see Section II-B) and Multimodal Semantic Comparator (MSC) (see Section II-C).

A. Transformer-based SLP Framework

To explore gloss semantic features, we build a transformer-based encoder. We apply a linear embedding layer to map

* Corresponding author.

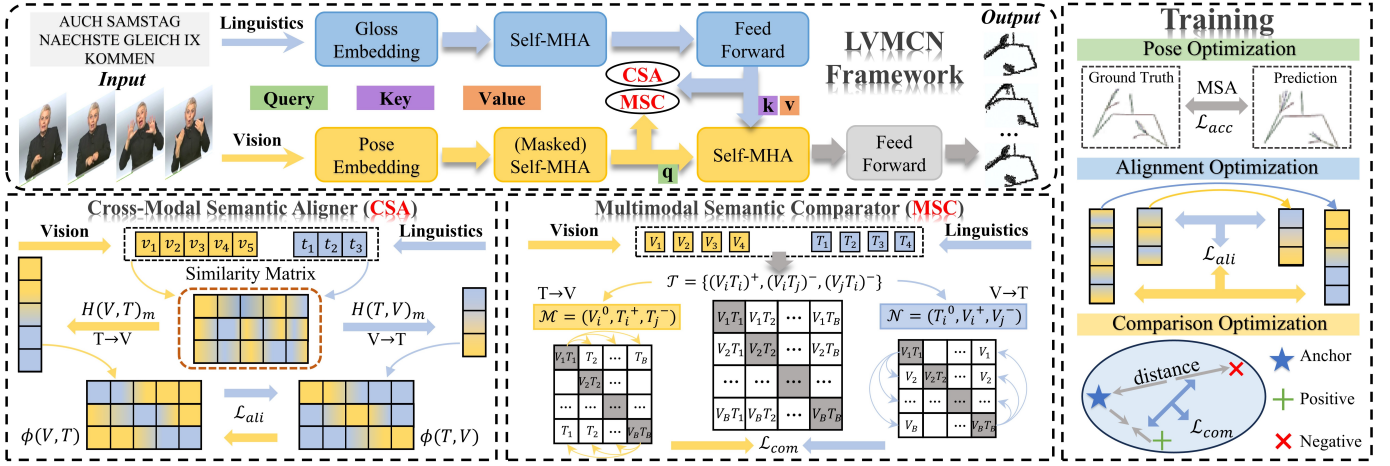


Fig. 1. Overview of LVMCN framework. It contains two key modules: Cross-modal Semantic Aligner (CSA) and Multimodal Semantic Comparator (MSC).

glosses into a high-dimensional space and a positional coding layer to capture temporal order, formulated as:

$$x'_n = W^g \cdot x_n + b^g + PE(n), \quad (1)$$

where x_n is a one-hot vector of the n -th gloss over the gloss vocabulary \mathcal{V} , PE is conducted by the sine and cosine functions on the temporal gloss order as in [12], and W^g and b^g represent the weight and bias respectively.

Then, we use Multi-Head Attention (MHA), Normalisation Layer (NL) and Feedforward Layer (FL) to capture the global semantics of the glosses, *i.e.*, $\tilde{x}'_{1:N} = NL(FL(MHA(x'_{1:N})))$.

Similar to the gloss encoding, we encode the sign poses into a high-dimensional feature space through a linear layer and a positional encoding layer PE' , formulated as:

$$y'_m = W^p \cdot y_m + b^p + PE'(m), \quad (2)$$

where y_m denotes the coordinates of the pose at m -th time stamp; W^p and b^p represent the weight and bias respectively.

Our pose decoder is recursive that predicts the next pose $\tilde{y}_{1:m}$ by aggregating all previously generated poses \tilde{y}_{m+1} . This process is formulated as follows:

$$\begin{aligned} \tilde{y}_{m+1} &= PoseDecoder(y'_{1:m}, \tilde{x}'_{1:N}) \\ \Leftrightarrow \begin{cases} z_m = FL(MHA_1(y'_{1:m}) + \tilde{y}_m), m \in [1, M]; \\ \tilde{y}_{m+1} = FL(MHA_2(z_m, \tilde{x}'_{1:N})), \end{cases} \end{aligned} \quad (3)$$

where MHA_1 and MHA_2 are the two layers of pose decoder.

Pose Optimization: In the training stage, the Mean Absolute Error (MAE) loss is used to constraint the consistency of the produced poses $\{\tilde{y}\}_{m=1}^M$ and the ground truth $\{\hat{y}\}_{m=1}^M$.

$$\mathcal{L}_{acc} = \frac{1}{M} \sum_{m=1}^M |\tilde{y}_m - \hat{y}_m|. \quad (4)$$

B. Cross-modal Semantic Aligner (CSA)

To achieve cross-modal monotonic matching between gloss and pose sequences, we design a fine-grained semantic aligner. Specifically, we automate the constraints on the implicit alignment between the corresponding gloss and pose sequences by computing the cosine similarity correlation matrices between the textual features $\{\tilde{x}\}_{n=1}^N$ and the visual features $\{z\}_{m=1}^M$ to

achieve accurate fine-grained cross-modal sequence monotonic alignment. In practice, we first normalize the textual features $\{\tilde{x}\}_{n=1}^N$ and visual features $\{z\}_{m=1}^M$, formulated as:

$$t_n = Normalize(\tilde{x}_n); v_m = Normalize(z_m). \quad (5)$$

We compute the match between t_n and v_t by cosine similarity and propose a textual visual semantic best matching function $\mathcal{H}(V, T)$, which finds the closest item from sequence $V = \{v_1, v_2, \dots, v_M\}$ for each item in sequence $T = \{t_1, t_2, \dots, t_N\}$. The calculation process can be expressed as:

$$\begin{cases} \mathcal{H}(V, T)_m = argmax(h(v_m, t_n)); \\ \phi(V, T) = \frac{1}{M} \sum_{m=1}^M h(v_m, \mathcal{H}(V, T)_m), \end{cases} \quad (6)$$

where $h(\cdot, \cdot)$ denotes cosine similarity. The result of $\phi(V, T)$ is the video-text similarity, which finds the most similar textual feature for each visual feature. We also calculate the text-video similarity $\phi(T, V)$ with the function $\mathcal{H}(T, V)$.

Alignment Optimization: For a batch containing B text-video pairs $\{V_i, T_i\}_{i=1}^B$, the alignment loss is defined as:

$$\begin{aligned} \mathcal{L}_{ali} &= -\frac{1}{B} \sum_{i=1}^B \left(\log \frac{\exp(\phi(V_i, T_i)/\tau)}{\sum_{j=1}^B \exp(\phi(V_i, T_j)/\tau)} \right. \\ &\quad \left. + \log \frac{\exp(\phi(T_i, V_i)/\tau)}{\sum_{j=1}^B \exp(\phi(T_i, V_j)/\tau)} \right) \end{aligned} \quad (7)$$

where $\phi(V_i, T_j)$ denotes the similarity of the i -th video to the j -th text, and $\phi(T_i, V_j)$ denotes the similarity of the i -th text to the j -th video. The temperature τ determines the degree of alignment between the gloss and pose sequences.

C. Multimodal Semantic Comparator (MSC)

To ensure global semantic consistency between textual sentences and sign videos, we propose a coarse-grained multimodal semantic comparator, which brings "positive" text-visual pairs closer together and pushes "negative" ones farther away in the metric space. Specifically, we first calculate the

TABLE I
QUANTITATIVE RESULTS ON PHOENIX14T DATASET. ‘†’ INDICATES THE MODEL IS TESTED BY US UNDER A FAIR SETTING.

Methods	DEV							TEST						
	B1↑	B4↑	ROUGE↑	WER↓	DTW-P↓	FID↓	MPJPE↓	B1↑	B4↑	ROUGE↑	WER↓	DTW-P↓	FID↓	MPJPE↓
Ground Truth	29.77	12.13	29.60	74.17	0.00	0.00	0.00	29.76	11.93	28.98	71.94	0.00	0.00	0.00
PT-base† [13]	9.53	0.72	8.61	98.53	29.33	2.90	41.92	9.47	0.59	8.88	98.36	28.48	3.22	51.35
PT-GN† [13]	12.51	3.88	11.87	96.85	11.75	2.98	40.63	13.35	4.31	13.17	96.50	11.54	3.33	50.80
NAT-AT [15]	–	–	–	–	–	–	–	14.26	5.53	18.72	88.15	–	–	–
NAT-EA [15]	–	–	–	–	–	–	–	15.12	6.66	19.43	82.01	–	–	–
D3DP-sign† [36]	17.20	5.01	17.94	91.51	–	2.38	39.42	16.51	5.25	17.55	91.83	–	2.63	47.65
DET [17]	17.25	5.32	17.85	–	–	–	–	17.18	5.76	17.64	–	–	–	–
G2P-DDM [37]	–	–	–	–	–	–	–	16.11	7.50	–	77.26	–	–	–
GCDM [16]	22.88	7.64	23.35	82.81	11.18	–	–	22.03	7.91	23.20	81.94	11.10	–	–
GEN-OBT [14]	24.92	8.68	25.21	82.36	10.37	2.54	41.47	23.08	8.01	23.49	81.78	10.07	2.97	52.90
LVMCN(Ours)	25.79	9.17	27.29	76.86	10.25	1.94	35.11	24.33	9.36	26.24	75.43	10.14	2.16	42.54

TABLE II
ABLATION RESULTS OF DIFFERENT MODULES ON PHOENIX14T.

Methods	DEV			TEST		
	B1↑	WER↓	FID↓	B1↑	WER↓	FID↓
w/o CSA&MSC	23.47	79.42	2.11	21.71	78.30	2.33
w/o CSA	23.92	77.53	2.07	22.98	76.16	2.21
w/o MSC	24.46	78.53	1.99	23.67	77.12	2.19
Full (Ours)	25.79	76.86	1.94	24.33	75.43	2.16

distance between gloss sequences $T = \{t_1, t_2, \dots, t_N\}$ and pose sequences $V = \{v_1, v_2, \dots, v_M\}$.

$$d(VT) = \frac{V^\top T}{\|V\| \|T\|} = L_2(V)^\top \cdot L_2(T) = VT, \quad (8)$$

where $d(VT)$ is the similarity score between features V and T , L_2 denotes L_2 -normalisation. Since the feature sequences V and T have been L_2 -normalised in CSA, the direct multiplication here is the similarity score of the sample pairs.

Then, we construct multimodal triplets from the batch data as $\mathcal{T} = \{(V_i T_i)^+, (V_i T_j)^-, (V_j T_i)^-\}$, where $(V_i T_i)^+$ represents a positive pair and $(V_i T_j)^-$ and $(V_j T_i)^-$ represent negative pairs. The distance measurement for positive and negative feature pairs must satisfy the following constraint:

$$\begin{cases} d(V_i T_i)^+ > d(V_i T_j)^- + \sigma; \\ d(V_i T_i)^+ > d(V_j T_i)^- + \sigma; \end{cases} \quad (9)$$

where σ controls the strength of comparison.

Comparison Optimization: For a batch containing B text-video pairs $\{V_i, T_i\}_{i=1}^B$, we divide the multimodal triplets $\mathcal{T} = \{(V_i T_i)^+, (V_i T_j)^-, (V_j T_i)^-\}$ into $\mathcal{M} = \{V_i^0, T_i^+, T_j^-\}$ and $\mathcal{N} = \{T_i^0, V_i^+, V_j^-\}$, where \mathcal{M} is used for text-visual comparisons and \mathcal{N} is used for visual-text comparisons. So the total comparison loss of the batch can be represented by:

$$\mathcal{L}_{com} = - \sum_{k \in K} \left(\sum_{m \in \mathcal{M}} h_m^k \log(p_m^k) + \sum_{n \in \mathcal{N}} h_n^k \log(p_n^k) \right), \quad (10)$$

where K is a unit matrix of dimension B and p_m^k and p_n^k are the results of Eq. 8, h_m and h_n represent one-hot coding of sample targets in triples \mathcal{M} and \mathcal{N} respectively.

In the end, to train the model in an end-to-end manner, the full objective function in this work is given as follows:

$$\mathcal{L} = \alpha \mathcal{L}_{acc} + \beta \mathcal{L}_{ali} + \gamma \mathcal{L}_{com}, \quad (11)$$

where α , β and γ are hyperparameters of equilibrium loss.

III. EXPERIMENTS

A. Experimental Settings

Dataset and Evaluation Metrics. Following existing works [13]–[15], [17], we evaluate our method on the German sign corpus PHOENIX14T [38], which is a widely used SLP dataset. Besides, the NSLT [38] is adopted as an offline back-translation evaluation tool. To measure the quality of our method we used BLEU, ROUGE, WER, DTW-P, FID and MPJPE, which are the most popular metrics in the SLP field.

Implementation Details. Since PHOENIX14T does not provide 3D skeleton labels, following [13], [15], we use OpenPose [39] to extract 2D joint coordinates. A skeletal correction model [5] is applied to convert 2D positions into 3D coordinates, which are regarded as the target pose. We build LVMCN in the transformer modules with 2 layers and 4 heads, where the embedding size is set to 512. In addition, we apply a Gaussian noise onto pose coordinates and the noise rate is set to 5. During training, we use the Adam optimizer with a learning rate 1×10^{-3} and set $\alpha = 1.0$, $\beta = 1 \times 10^{-7}$, $\gamma = 1 \times 10^{-5}$, $\tau = 0.01$, $\sigma = 0.05$. Our code implemented PyTorch on NVIDIA GeForce RTX 2080 Ti GPU.

B. Comparison with State-of-the-Arts

As shown in Table I, LVMCN performs prominent superiority to all the other methods. Compared with the transformer-based baseline **PT-base**, our method improves 16.26% and 14.86% for BLEU-1 on DEV and TEST, respectively. And compared with the upgraded transformer method **PT-GN**, our method is still superior in all metrics, such as WER (reducing by 19.99%/21.07%). For the graph-based models, **NAT-AT** and **NAT-EA** have just reported the TEST set experimental results. Compared with the best version **NAT-EA** is obviously far behind ours (weakening 2.70% on BLEU-4). Besides, our method outperforms another transformer-based method **DET** too (raising 9.44%/8.60% for ROUGE on DEV/TEST). Furthermore, compared with **D3DP-sign**, **G2P-DDM** and **GCDM**, which are based on the most popular diffusion modeling method, our method also achieves better performance on TEST set (enhances 7.82%/8.22%/2.30% on BLEU-1 and 4.11%/1.86%/1.45% on BLEU-4). In the end, we compare with the best-performing method **GEN-OBT**. Only the DTW-P is slightly worse 0.07 on TEST, while all other metrics are substantially higher than those of the GEN-OBT.

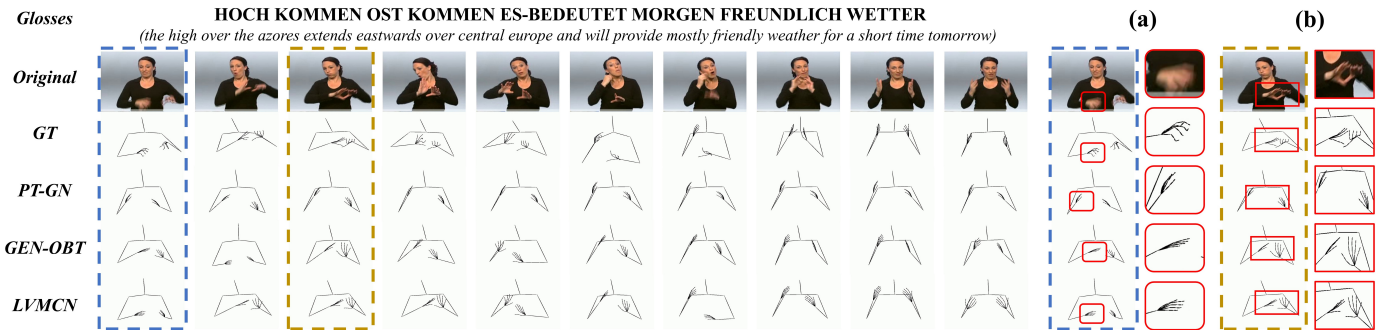


Fig. 2. Visualization examples of produced pose sequence. We compare our LVMCN with PT-GN and GEN-OBT. Here, (a) show that LVMCN generates close-to-natural arm poses under labeling errors, while (b) show the cases that LVMCN fits the original frame better than ground-truth.

TABLE III
ABLATION RESULTS OF PARAMETERS ON PHOENIX14T.

Methods	DEV			TEST		
	B1 \uparrow	WER \downarrow	FID \downarrow	B1 \uparrow	WER \downarrow	FID \downarrow
τ	0.01	25.79	76.86	1.94	24.33	75.43
	0.10	23.38	78.41	1.99	22.85	78.68
	1.00	22.00	80.78	2.13	21.86	79.64
σ	0.01	24.25	80.73	2.04	23.05	80.42
	0.05	25.79	76.86	1.94	24.33	75.43
	0.10	24.30	77.24	1.95	22.08	76.97

C. Ablation Study

Ablations of Modules. Table II shows the ablation results of CSA and MSC. We set a transformer-based baseline **w/o CSA&MSC**, in which the poses are generated only under L_{acc} constraint. **w/o CSA** refers to MSC is applied into baseline, which enhances 0.45%/1.27% BLEU-1 and reduces 1.89%/2.14% WER on DEV/TEST, respectively. **w/o MSC** refers to CSA is applied into baseline, which leads to obvious improvement too (e.g., 1.96% BLEU-1, 0.14 FID on TEST). Moreover, our method **Full (Ours)** achieves the best performance in all back-translation metrics, which indicates that the introduced CSA and MSC improve cross-modal semantic associations between linguistic and visual cues.

Analysis of Parameters. Table III shows ablation results of parameters, containing the similarity τ and contrast σ during training. We gradually increase the above parameters to test and the results show that our model performs best when $\tau = 0.01$ and $\sigma = 0.05$.

D. Qualitative Results

Visualization of Generated Example. Figure 2 provides the pose examples generated by the PT-GN [13] and GEN-OBT [14] to demonstrate the superiority of the LVMCN. For examples (a) with noise labels labelling the original video blur, our method generates poses that are closest to natural. For the poses shown with pose labels (b) that deviate from the original video, our LVMCN generates poses that are more realistic than PT-GN and GEN-OBT and are closer to the real video.

Instantiation of Fine-grained Alignment. Figure 3 shows example of cross-modal fine-grained alignment in CSA. As shown in this figure, the highly responsive attention regions are diagonally distributed in the attention map proving that our model achieves fine-grained semantic monotonic alignment. Additionally, we observe that some adjacent highly

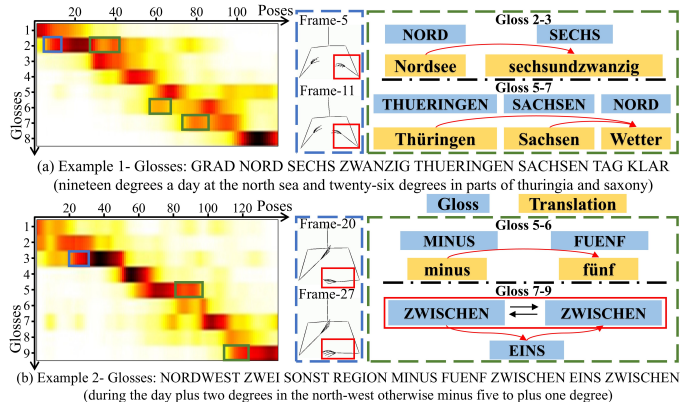


Fig. 3. The result of fine-grained alignment in the CSA.

responsive attention regions temporally overlap, which is a reasonable phenomenon. On the one hand, consecutive small-amplitude movements will represent multiple discrete sign language words, and our model excels at fine-grained semantic alignment, which results in multiple glosses corresponding to adjacent poses (blue box). On the other hand, LVMCN can capture multiple words with semantic continuity, causing overlapping high-response attentional regions (green box).

IV. CONCLUSIONS

This work proposes a linguistics-vision monotonic consistent network for SLP, which includes a fine-grained Cross-modal Semantic Aligner (CSA) and a coarse-grained Multimodal Semantic Comparator (MSC). Specifically, CSA computes a similarity matrix to align sign glosses with actions. MSC constructs multimodal triples from paired and unpaired data, improving semantic consistency by bringing corresponding text-visual pairs closer and separating non-corresponding ones. Experiments validate the effectiveness of the method.

ACKNOWLEDGMENT

This work was supported by the National Natural Science Foundation of China (Grants No. U23B2031, 61932009, U20A20183, 62272144, 62402471), the Anhui Provincial Natural Science Foundation, China (Grant No. 2408085QF191), the Fundamental Research Funds for the Central Universities (Grant No. JZ2024HGTA0178), the Major Project of Anhui Province (Grant No. 202423k09020001), and the China Post-doctoral Science Foundation (Grant No. 2024M763154).

REFERENCES

- [1] Kostas Karpouzis, George Caridakis, S-E Fotinea, and Eleni Efthimiou, “Educational resources and implementation of a greek sign language synthesis architecture,” *Computers & Education*, vol. 49, no. 1, pp. 54–74, 2007.
- [2] Dimitris Kouremenos, Klimis S Ntalianis, Giorgos Siolas, and Andreas Stafylopatis, “Statistical machine translation for greek to greek sign language using parallel corpora produced via rule-based machine translation,” in *International Conference on Tools with Artificial Intelligence*, 2018, pp. 28–42.
- [3] Jan Zelinka, Jakub Kanis, and Petr Salajka, “Nn-based czech sign language synthesis,” in *International Conference on Speech and Computer*, 2019, pp. 559–568.
- [4] Feng Li, Yixuan Wu, Anqi Li, Huihui Bai, Runmin Cong, and Yao Zhao, “Enhanced video super-resolution network towards compressed data,” *ACM Transactions on Multimedia Computing, Communications and Applications*, pp. 1–21, 2024.
- [5] Jan Zelinka and Jakub Kanis, “Neural sign language synthesis: Words are our glosses,” in *Winter Conference on Applications of Computer Vision*, 2020, pp. 3395–3403.
- [6] Feng Li, Runmin Cong, Jingjing Wu, Huihui Bai, Meng Wang, and Yao Zhao, “Srconvnet: A transformer-style convnet for lightweight image super-resolution,” *International Journal of Computer Vision*, pp. 1–17, 2024.
- [7] Shyam Krishna and Janmesh Ukey, “Gan based indian sign language synthesis,” in *Indian Conference on Vision, Graphics and Image Processing*, 2021, pp. 1–8.
- [8] Neel Vasani, Pratik Autee, Samip Kalyani, and Ruhina Karani, “Generation of indian sign language by sentence processing and generative adversarial networks,” in *International Conference on Information Systems Security*, 2020, pp. 1250–1255.
- [9] Euijun Hwang, Jung-Ho Kim, and Jong-Cheol Park, “Non-autoregressive sign language production with gaussian space,” in *British Machine Vision Conference*, 2021, pp. 1–13.
- [10] Qinkun Xiao, Mingyong Qin, and Yuting Yin, “Skeleton-based chinese sign language recognition and generation for bidirectional communication between deaf and hearing people,” *Neural Networks*, vol. 125, pp. 41–55, 2020.
- [11] Shengeng Tang, Jiayi He, Dan Guo, Yanyan Wei, Feng Li, and Richang Hong, “Sign-idd: Iconicity disentangled diffusion for sign language production,” in *AAAI Conference on Artificial Intelligence*, 2025.
- [12] Ashish Vaswani, Noam Shazeer, Niki Parmar, Jakob Uszkoreit, Llion Jones, Aidan N Gomez, Łukasz Kaiser, and Illia Polosukhin, “Attention is all you need,” in *Neural Information Processing Systems*, 2017, pp. 1–11.
- [13] Ben Saunders, Necati Cihan Camgoz, and Richard Bowden, “Progressive transformers for end-to-end sign language production,” in *European Conference on Computer Vision*, 2020, pp. 687–705.
- [14] Shengeng Tang, Richang Hong, Dan Guo, and Meng Wang, “Gloss semantic-enhanced network with online back-translation for sign language production,” in *ACM International Conference on Multimedia*, 2022, pp. 5630–5638.
- [15] Wencan Huang, Wenwen Pan, Zhou Zhao, and Qi Tian, “Towards fast and high-quality sign language production,” in *ACM International Conference on Multimedia*, 2021, pp. 3172–3181.
- [16] Shengeng Tang, Feng Xue, Jingjing Wu, Shuo Wang, and Richang Hong, “Gloss-driven conditional diffusion models for sign language production,” *ACM Transactions on Multimedia Computing, Communications, and Applications*, 2024.
- [17] Carla Viegas, Mert Inan, Lorna Quandt, and Malihe Alikhani, “Including facial expressions in contextual embeddings for sign language generation,” in *Joint Conference on Lexical and Computational Semantics*, 2023, pp. 1–10.
- [18] Cong Hu, Biao Fu, Pei Yu, Liang Zhang, Xiaodong Shi, and Yidong Chen, “An explicit multi-modal fusion method for sign language translation,” in *IEEE International Conference on Acoustics, Speech and Signal Processing*. IEEE, 2024, pp. 3860–3864.
- [19] Biao Fu, Peigen Ye, Liang Zhang, Pei Yu, Cong Hu, Xiaodong Shi, and Yidong Chen, “A token-level contrastive framework for sign language translation,” in *IEEE International Conference on Acoustics, Speech and Signal Processing*. IEEE, 2023, pp. 1–5.
- [20] Rui Zhao, Liang Zhang, Biao Fu, Cong Hu, Jinsong Su, and Yidong Chen, “Conditional variational autoencoder for sign language translation with cross-modal alignment,” in *Association for the Advancement of Artificial Intelligence*, 2024, pp. 19643–19651.
- [21] Shengeng Tang, Dan Guo, Richang Hong, and Meng Wang, “Graph-based multimodal sequential embedding for sign language translation,” *IEEE Transactions on Multimedia*, vol. 24, pp. 4433–4445, 2021.
- [22] Jingjing Wu, Yunkai Zhang, Xi Zhou, Shengeng Tang, and Yanyan Wei, “Comprehensive survey on person identification: Queries, methods, and datasets,” in *ICMR Workshop on Multimedia Object Re-Identification*, 2024, pp. 1–6.
- [23] Liwei Wang, Yin Li, Jing Huang, and Svetlana Lazebnik, “Learning two-branch neural networks for image-text matching tasks,” *IEEE Transactions on Pattern Analysis and Machine Intelligence*, vol. 41, no. 2, pp. 394–407, 2018.
- [24] Jingjing Wu, Richang Hong, and Shengeng Tang, “Intermediary-generated bridge network for rgb-d cross-modal re-identification,” *ACM Transactions on Intelligent Systems and Technology*, vol. 15, no. 6, pp. 1–25, 2024.
- [25] Liangli Peng, Peng Hu, Xu Wang, and Dezhong Peng, “Deep supervised cross-modal retrieval,” in *Computer Vision and Pattern Recognition*, 2019, pp. 10394–10403.
- [26] Yaxiong Wang, Hao Yang, Xiuxiu Bai, Xueming Qian, Lin Ma, Jing Lu, Biao Li, and Xin Fan, “Pfan++: Bi-directional image-text retrieval with position focused attention network,” *IEEE Transactions on Multimedia*, vol. 23, pp. 3362–3376, 2020.
- [27] Yuting Ma, Shengeng Tang, Xiaohua Xu, and Lechao Cheng, “Modality alignment meets federated broadcasting,” *arXiv preprint arXiv:2411.15837*, 2024.
- [28] Qingbao Huang, Jielong Wei, Yi Cai, Changmeng Zheng, Junying Chen, Ho-fung Leung, and Qing Li, “Aligned dual channel graph convolutional network for visual question answering,” in *Association for Computational Linguistics*, 2020, pp. 7166–7176.
- [29] Yanyan Wei, Yilin Zhang, Kun Li, Fei Wang, Shengeng Tang, and Zhao Zhang, “Leveraging vision-language prompts for real-world image restoration and enhancement,” *Computer Vision and Image Understanding*, vol. 250, pp. 104222, 2025.
- [30] Pin Jiang and Yahong Han, “Reasoning with heterogeneous graph alignment for video question answering,” in *Association for the Advancement of Artificial Intelligence*, 2020, pp. 11109–11116.
- [31] Peipei Song, Dan Guo, Xun Yang, Shengeng Tang, Erkun Yang, and Meng Wang, “Emotion-prior awareness network for emotional video captioning,” in *Proceedings of the 31st ACM International Conference on Multimedia*, 2023, pp. 589–600.
- [32] Xingwei Tan, Yi Cai, Jingyun Xu, Ho-Fung Leung, Wenhao Chen, and Qing Li, “Improving aspect-based sentiment analysis via aligning aspect embedding,” *Neurocomputing*, vol. 383, pp. 336–347, 2020.
- [33] Juhua Liu, Qihuang Zhong, Liang Ding, Hua Jin, Bo Du, and Dacheng Tao, “Unified instance and knowledge alignment pretraining for aspect-based sentiment analysis,” *IEEE/ACM transactions on audio, speech, and language processing*, vol. 31, pp. 2629–2642, 2023.
- [34] Cheng Ye, Weidong Chen, Jingyu Li, Lei Zhang, and Zhendong Mao, “Dual-path collaborative generation network for emotional video captioning,” in *Proceedings of the 32nd ACM International Conference on Multimedia*, 2024, pp. 496–505.
- [35] Peipei Song, Dan Guo, Xun Yang, Shengeng Tang, and Meng Wang, “Emotional video captioning with vision-based emotion interpretation network,” *IEEE Transactions on Image Processing*, vol. 33, pp. 1122–1135, 2024.
- [36] Wenkang Shan, Zhenhua Liu, Xinfeng Zhang, Zhao Wang, Kai Han, Shanshe Wang, Siwei Ma, and Wen Gao, “Diffusion-based 3d human pose estimation with multi-hypothesis aggregation,” in *IEEE/CVF International Conference on Computer Vision*, 2023, pp. 14761–14771.
- [37] Pan Xie, Qipeng Zhang, Peng Taiying, Hao Tang, Yao Du, and Zexian Li, “G2p-ddm: Generating sign pose sequence from gloss sequence with discrete diffusion model,” in *Association for the Advancement of Artificial Intelligence*, 2024, pp. 6234–6242.
- [38] Necati Cihan Camgoz, Simon Hadfield, Oscar Koller, Hermann Ney, and Richard Bowden, “Neural sign language translation,” in *Computer Vision and Pattern Recognition*, 2018, pp. 7784–7793.
- [39] Zhe Cao, Tomas Simon, Shih-En Wei, and Yaser Sheikh, “Realtime multi-person 2d pose estimation using part affinity fields,” in *Computer Vision and Pattern Recognition*, 2017, pp. 7291–7299.